

Journal of **Fisheries and Aquatic Science**

ISSN 1816-4927



Riverine Flow Sediment Exclusion Using Vortex Chamber

Gheisi Ali Reza and Keshavarzi Ali Reza Department of Water, Shiraz University, Shiraz, Iran

Abstract: In this study an effort was made to understand flow structure and in particular secondary currents inside the vortex chamber. To study the flow structure inside the vortex chamber, the three dimensional flow velocity in tangential, radial and vertical directions were measured using Acoustic Doppler Velocity meter (ADV). The velocity was measured in 384 different nodal points, at eight different layers within the flow depth and at the radius of 0, 45, 90, 135, 180, 225, 270 and 315 degree. From this study, it was found that some symmetrical contour lines exist near the bed of the chamber. Additionally some secondary currents were recognized inside the vortex chamber and particularly around the overflow weir and inlet jet. The above information about the secondary current helps for numerical modeling and also to design a new chamber with higher trap efficiency than previously proposed settling basin by strengthening the useful secondary currents and removing the usefulness ones.

Key words: Flow structure, sedimentation tank, vortex chamber, self-flushing tank, secondary currents

Introduction

One of the major concerns for the hydraulic engineers is to exclude sediment particles from the stream flow. The vortex chamber is normally used to exclude sediment particles from the diverted water. In vortex chamber, the vortex of flow and secondary currents are used to exclude suspended sediment particles from the flow. In vortex chamber, a combined vortex (Rankine type vortex) with a forced vortex near the orifice, a free vortex in the outer region and in the periphery of the chamber is formed. The secondary flow develops as a result of the flow deceleration at the bottom of the vortex chamber. These secondary currents cause the near periphery wall flow to move toward the floor of the chamber and finally deflect toward the central flushing orifice.

The variation of sediment concentration within the vortex chamber is greatly affected by variation of velocity components in vertical, radial and tangential flow directions. A number of studies for example by Cecen and Bayazit (1975), Odgaard (1986), Hite and Mih (1994), Salakhov (1975) and Ogihara and Sakaguchi (1984) have attempted to find the velocity variations inside the vortex chamber. From the above studies, it was found that the flow pattern in the vortex chamber is comparatively similar to the flow pattern in a combined vortex system. Also it was found that the flow pattern is highly affected by the inlet and outlet flow condition. Rea (1984) studied the flow structure and in particular the secondary currents pattern inside a vortex chamber. Variation of velocity components in the vortex chamber was also studied by Curi *et al.* (1979), Mashauri (1986), Paul *et al.* (1991),

Julien (1986), Vatistas (1989) and Zhou *et al.* (1997). From these studies it was found that the tangential and radial velocities remained almost uniform over the flow depth in the vortex chamber. The variation of vertical velocity is only significant at the near the central orifice. Athar *et al.* (2003) measured the flow velocity in two dimensions including tangential and radial directions in a horizontal plane within the vortex chamber and found some information for the horizontal velocity components. From the above study it was found that the flow structure in the segments of the vortex chamber are highly affected with inlet and outlet flow conditions and did not compare well with the Rankine vortex. However, they pointed out that the presented information is only useful for the used basin type used in their study and is not applicable to other geometries. Also the presented information for the segments can not define the flow structure at the sections in the radius of the chamber due to limitation for velocity measurement in three dimensions. As the flow in a chamber is three dimensional, therefore, this study is focused on the measurement of flow velocity in three dimensional and in particular at each section of flow in the radius inside the chamber.

Materials and Methods

The experimental tests were performed in a physical model which was built in hydraulic laboratory of water department, Shiraz University, Shiraz, Iran. The chamber model was cylindrical with the diameter of 1.00 m and height of 0.70 m. The model enables to perform the tests in clockwise and anticlockwise flow directions. In anticlockwise flow direction, the angular distance from the inlet channel to the outlet overflow weir is about 270 degree. A diaphragm is also provided at the inlet. The diaphragm was installed at 0.17 m from the bed at the periphery of the basin. The width of the inlet canal was 0.20 m with the slope of 0.01. A flushing pipe was installed at the center of the chamber with a diameter of 0.05 m. The basin bed was sloped into the central flushing orifice. The chamber's depth at its periphery was 0.60 m. The length of the overflow weir was 0.50 m. A schematic diagram of the chamber is shown in Fig. 1.

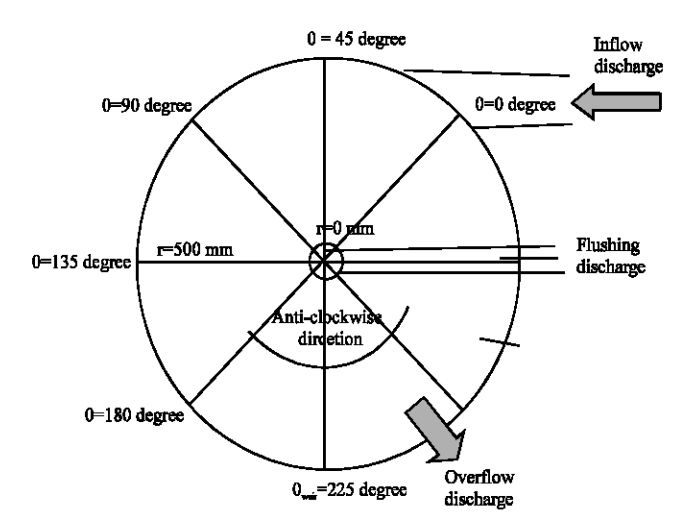


Fig. 1: Plane view of the vortex chamber

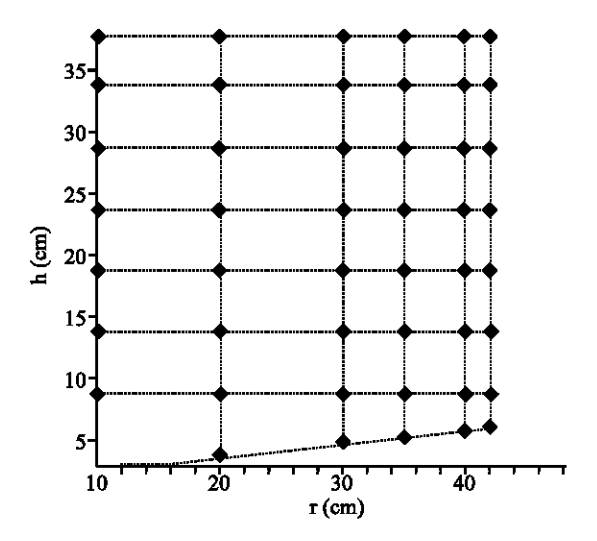


Fig. 2: Radius cross section of flow inside chamber

To measure flow rate at the outlet of flushing orifice and overflow weir, two pre-calibrated right angle V-notches were installed at the outlet of the model. To calibrate V-notches, an accurate apparatus was used to measure time and volume of the flow. The calibrating apparatus consists of two electronic level controllers and two specific sensors with digital timer. Using this apparatus allows us to pump 15 cubic meters of water in a time period. Thus, the flow rate is accurately measured over the weir.

The velocity of flow in three dimensions was measured using ADV (Acoustic Doppler Velocity meter) in 384 different nodal points, formed at eight different elevations through eight angles. The flow streamlines were plotted in eight radial sections with angular distance of 45 degree. In each section velocities were measured in 48 points. Figure 2 shows the position of the radius sections and the grid of data acquisition in each section.

Results and Discussion

As mentioned previously, in some studies for example; Rea (1984) and Athar *et al.* (2003), it was recognized that the secondary currents in the vortex chamber is very effective to increase the efficiency of the vortex chamber. As a result, in this study an effort was made to understand the flow mechanism and especially secondary currents in a physical model of a vortex chamber in fully three dimensional forms. The physical model in this study was constructed on the basis of the previous suggestions which were made by Sullivan (1972), Cecen and Bayazit (1975), Salakhov (1975), Chrysostomou (1983), Mashauri (1986) and Paul *et al.* (1991). Therefore to understand flow structure inside a vortex chamber the three dimensional flow velocities were measured using ADV. The results of the flow streamlines in tangential, radial and vertical directions are presented in Fig. 3a-f for different angles. The flow structure for eight sections in radial and at eight angles of 0, 45, 90, 135, 180, 225, 270 and 315 degree is presented and they are discussed in the following sections.

Flow Streamlines and Secondary Currents at Different Radial Sections Inside the Vortex Chamber Secondary Currents at $\theta = 0$ degree Radial Section

This section is located exactly in front of inlet flow. In this section most of streamlines are deflected towards the center of the chamber and as a result some secondary currents are formed. A vortex is formed at the top of flow inlet from elevation h=0.5R to the water surface whereas another vortex appears exactly under the flow inlet from h=0.3R to the bottom of the chamber. This section is the location where most vortices initiate to form. As a result, it was found that two vortices are formed on the top and bottom of the inlet jet flow (Fig. 3a).

Secondary Currents at $\theta = 45$ degree Radial Section

At this section the vortices which initiated to form at 0° are changed into two complete vortices. The upper vortex rotates in clockwise direction whereas the near bed vortex rotates in anticlockwise direction. Figure 3b shows that the flow in this section is influenced highly by the inlet jet and the vortices are produced as a result of the inlet jet performance. In the near bed vortex, the streamlines are rotating in anticlockwise direction and move the near bed current towards the central flushing orifice. The upper vortex is very powerful and produced a region with high upward tendency. The other streamlines that are not confined by these two vortices move towards the center of the chamber (Fig. 3b).

Secondary Currents at $\theta = 90$ degree Radial Section

This section is located far from the inlet, the influence of the inlet jet decreases significantly and some changes happen abruptly. The two vortices in the previous section are changed into three vortices at this section. The third vortex appears exactly at the upper portion, near the center of chamber and rotates in anticlockwise direction. By tracing the developed stage of this vortex in the subsequent sections, it was found that its formation is caused by the overflow weir, which is 135° far from this section. Also it was found that the tendency of streamlines direction towards the weir starts before the flow reaches the overflow weir. The generated vortex has great influence on the other two vortices. For example it stretches down the previous upper vortex towards the bed and also develops this vortex downward by confining it between two vortices. The streamlines with a great tendency towards the center of chamber cover the larger portion of the flow domain in the previous section. But by the effect of this new vortex this tendency is restricted only at elevation between the bed and h = 0.4R. It shows that formation of the new third vortex will make streamlines run away from the center of chamber. It is obvious that the rotational direction of the upper inlet jet vortex which was formed by the effect of the inlet jet will help the third vortex in its formation and developing at this section (Fig. 3c).

Secondary Currents at $\theta = 135$ degree Radial Section

Close to the overflow weir, the third vortex which was formed in the 90 degree section is now developing and occupies approximately 50% of the area at 135 degree section. The upper vortex which was formed by the action of the inlet jet is small at this section and forced towards the periphery wall of the chamber. The near bed vortex which made a current towards the central orifice, now is dividing into two small vortices because its flow direction was opposite to the predominant current. At the position where the near bed current gets close to the predominant current, a new vortex is appeared in clockwise direction. It is also observed that most streamlines flow directions in this section is towards the chamber's periphery especially near the central air core (Fig. 3d).

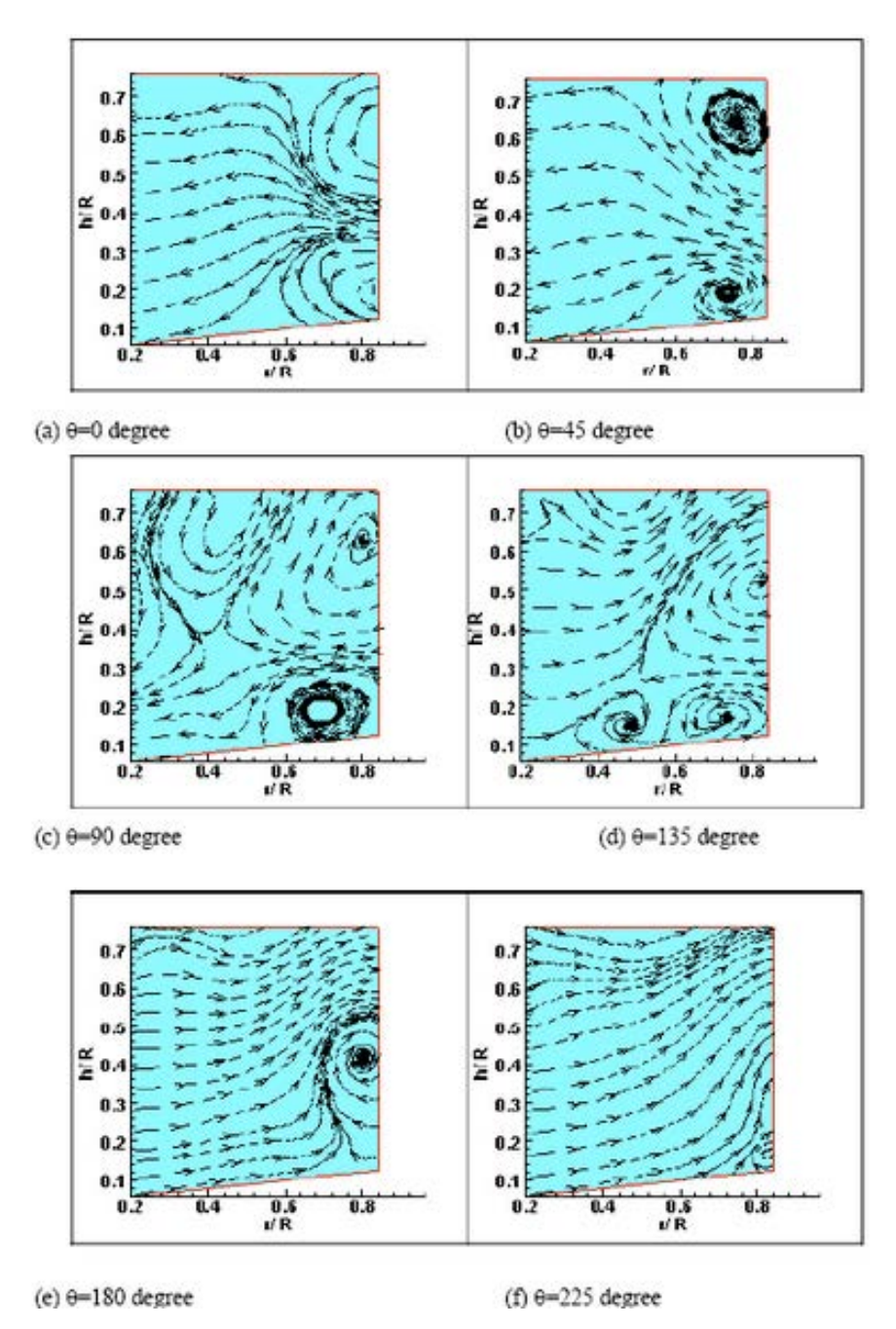


Fig. 3: Streamlines of flow at 0, 45, 90, 135, 180 and 225 degree cross sections in the chamber

Secondary Currents at $\theta = 180$ degree Radial Section

In this section the predominant currents which produced in the previous section, developed to fill most part of this section. It is shown in Fig. 2e that the streamlines of the predominant currents moved towards the overflow weir and pull the upper vortex downward. Then confines it between the bed and the elevation equal to h = 0.5R. Therefore, at this section all the streamlines are deflected towards the overflow weir (Fig. 3e). Also, the secondary currents at $\theta = 225^{\circ}$ radial section, which is located exactly close to the overflow weir, all streamlines in this section move toward the top of the weir except a small vortex which is remained at the corner of chamber's periphery (Fig. 3f).

Distribution of Tangential Velocity at Different Radial Sections Inside the Vortex Chamber Variation of Tangential Velocity at $\theta = 0$ degree Radial Section

It is observed that exactly at the inlet portion where the water enters into the chamber there is a circular region with the radius equal to half of the distance between the center of the upper and near bed vortices. In free vortex condition, by getting close to the center of vortex, the tangential velocity was increased. But in front of the flow inlet, the flow structure is highly influenced by the inlet jet and the tangential velocity is abruptly increased. Another significant change in the tangential velocity distribution was found in the vicinity of the central air core. It can be seen that at the radius equal to r = 0.2R to 0.4R a steep gradient of tangential velocity toward the center of the vortex chamber is occurred (Fig. 4a).

Variation of Tangential Velocity at $\theta = 45$ degree Radial Section

From the contour lines, two regions with high value of tangential velocity are clear at this section and they are located in the middle of the section and around the center of chamber. In the region close to the center of chamber, the tangential velocity increases from the wall to the center. Also the tangential velocity increases in vertical direction and from the bed to the water surface. Therefore, the highest value of tangential velocity occurred at the coordinate of r=0.2R and h=0.6R and it occurred close to the water surface and at the center of the chamber. The other region with high value of tangential velocity which is formed by the effect of the inlet flow is located between the radius of r=0.5R to 0.7R (Fig. 4b). As a result, it was found that by increasing the angular distance from the inlet orifice the inlet jet will deflect towards the center of the vortex chamber.

Variation of Tangential Velocity at $\theta = 90$ degree Radial Section

The region with high tangential velocity which was formed as a result of the inlet jet in the previous section is disappeared in this section. Therefore, there was no effect of the inlet jet in this section. The third vortex which appears in this section is very effective to stretch the flow towards the periphery of the chamber and in upward direction. As a result, at this section the contour lines of the tangential velocities are bulged in upward direction towards the water surface. Therefore, a region with steep gradient of the tangential velocity is produced at a region close to the water surface (Fig. 4c).

Variation of Tangential Velocity at $\theta = 135^{\circ}$ Radial Section

Comparing to the 90° section, it was found that at this section by approaching towards the overflow weir approximately all the contour lines of the tangential velocities are bulged in upward direction towards the overflow weir. The region with higher tangential velocity is appeared in vicinity of the chamber center at r = 0.2R and very close to the water surface (Fig. 4d).

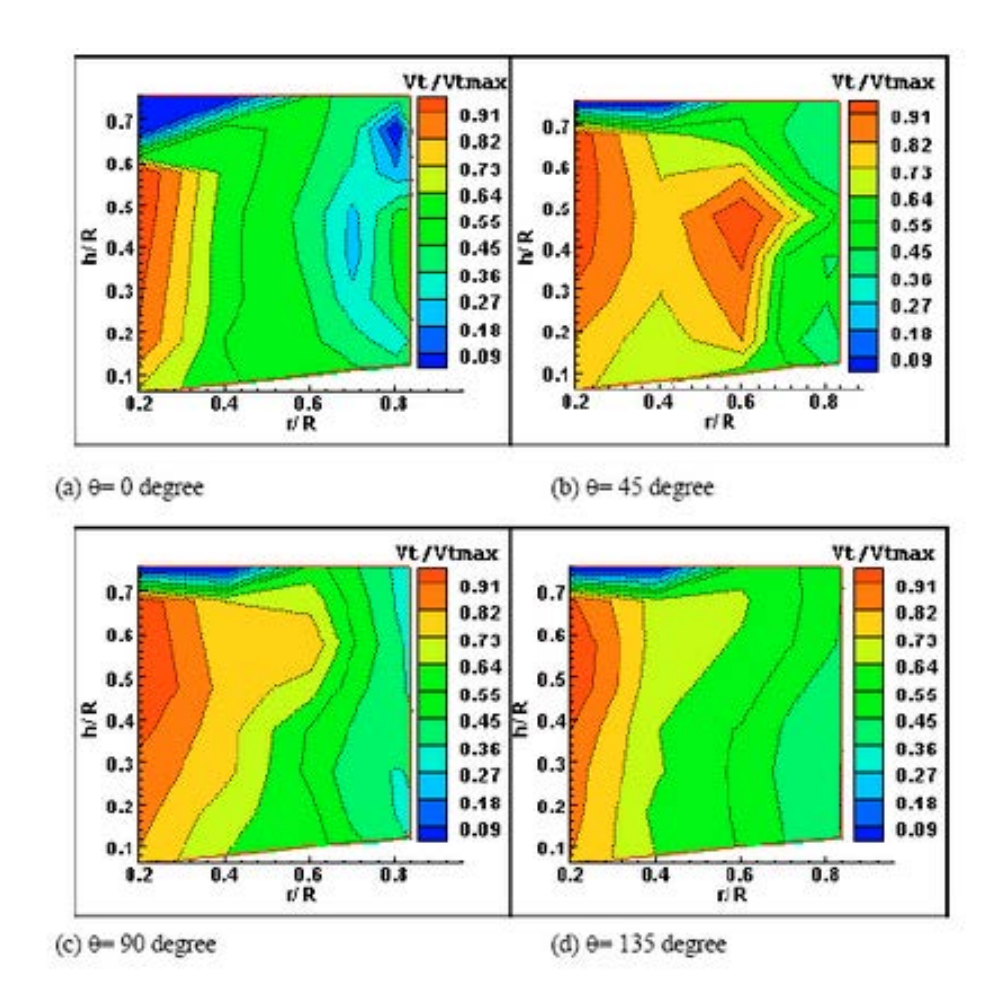


Fig. 4: The tangential velocity at 0, 45, 90 and 135 degree cross sections in the Chamber

Distribution of Radial Velocity at Different Radial Sections Inside the Vortex Chamber

Figure 5a-d shows the contour lines of the radial velocity which is normalized by maximum tangential velocity (V_r/V_{truex}) in radial sections $\theta=0$ to 135 degree. Also the regions with inward velocities are separated from the regions with outward velocities with solid dark lines (Fig. 5a-d).

Variation of Radial Velocity at θ = 0 degree Radial Section

The radial velocity at this section is very much influenced by the inlet jet and three regions at this section were recognized. The first region is located exactly in front of the inlet jet and can be separated from the other regions by drawing a circle with radius equal to half of the distance between center of the upper and near bed vortices. The maximum inward velocity occurred at the center of this region. At the center of this region the inward velocity increased to 63% of the maximum tangential velocity. It can be seen that at this circular region by getting far from the center towards the periphery, the inward velocity was rapidly decreased. This is due to that the upper inlet jet is greatly under the

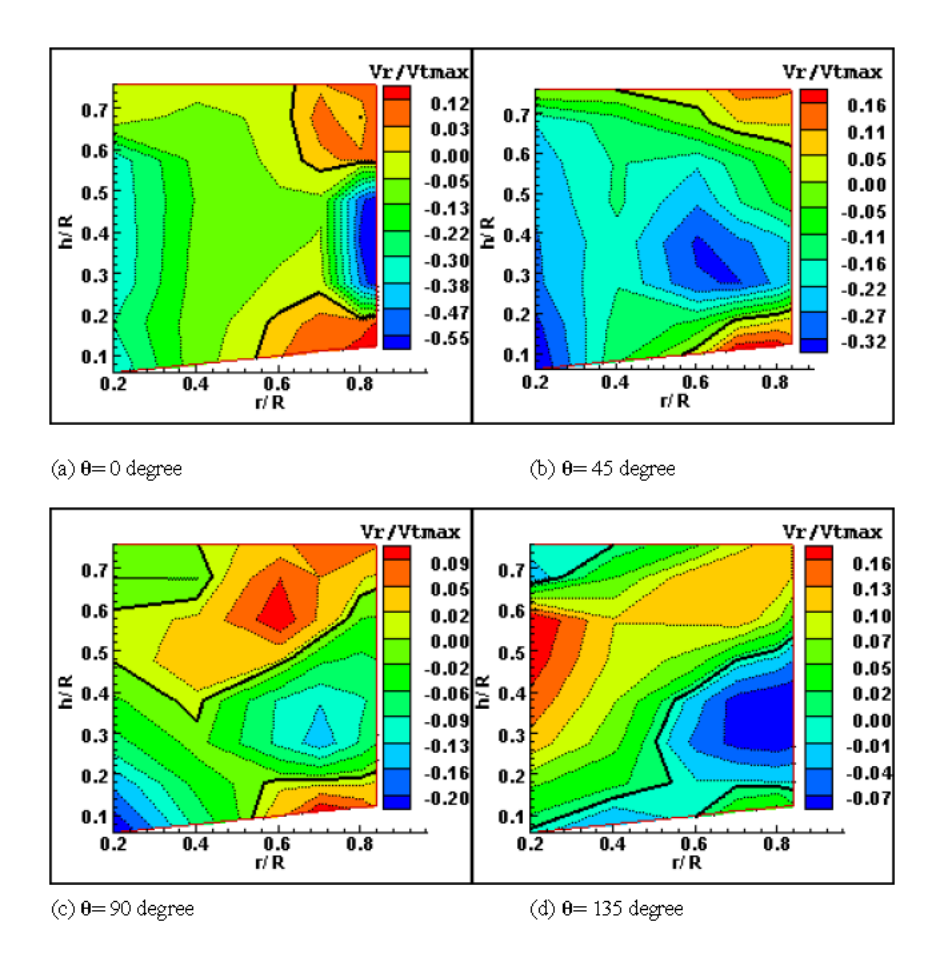


Fig. 5: The radial velocity at 0, 45, 90 and 135 degree cross sections in the Chamber

influence of the two vortices towards the center of chamber. Therefore, at the center of this circular region of flow is moved towards the center of chamber. The second region is located at the radius of r = 0.6R to 0.2R from the central orifice. In this region by getting close to the center of the chamber, the inward velocity increased towards the central orifice. The only region where the value of radial velocity is positive is the chamber's periphery. The maximum value of the outward velocity occurred under the near bed vortex and at the corner of the chamber and it is 20% of the maximum tangential velocity (Fig. 5a).

Variation of Radial Velocity at θ = 45 degree Radial Section

The value of the radial velocity in the whole section is negative except the regions under the near bed vortex and over the upper vortex. It was found that from radius r=0.84R to r=0.6R toward the central orifice, the inward velocity increased to 33% of the maximum tangential velocity at this section. Hence the tendency of streamlines towards the center of the chamber was increased. From the radius

of r=0.6R to r=0.4R, the inward velocity is suddenly decreased. The tendency of streamlines towards the center of chamber increased from radius r=0.4R to r=0.2R. The inward velocity increased to its maximum value in vicinity of the central flushing orifice and it is about 37% of the maximum tangential velocity. Additionally, it was found that the near bed and the upper inlet jet vortices are the forced vortices. The maximum value of the outward velocity occurred beneath the near bed at r=0.7R. It was 21% of the maximum tangential velocity (Fig. 5b).

Variation of Radial Velocity at $\theta = 90$ degree Radial Section

In this section the new vortex was appeared near the center of the chamber. The region with outward velocity was formed over the upper vortex and it is developed over a large part of this section. Similarly to the previous section, a region with the same distribution of radial velocity was found between the two near bed and upper vortices but it stretched downward. The region with high gradient variation of radial velocity which was located next to the center of chamber is pushed downward towards the central orifice. Hence, the maximum inward velocity occurred in the vicinity of the central orifice and it was 23% of the maximum tangential velocity. Similar to the previous section the maximum value of the outward velocity occurred beneath the near bed vortex at r=0.7R but it was 12% of the maximum tangential velocity (Fig. 5c).

Variation of Radial Velocity at $\theta = 135$ degree Radius Section

As approaching to the overflow weir the development of the third vortex was formed. As a result a region with outward velocity was found above a region with downward radial velocity. The upper region deflects the streamlines toward the overflow weir with the maximum outward velocity of $V_r = 0.19 V_{\text{tmsec}}$ near the center of the chamber. The lower region deflects the streamlines towards the central flushing orifice with the maximum inward velocity of $V_r = 0.1 V_{\text{tmsec}}$ close to the periphery wall of the vortex chamber.

Distribution of Radial Velocity at Different Horizontal Flow Levels Radial Velocity Distribution near the Bed

The value of radial velocities in the near bed shows that some anti-symmetrical patterns were formed. Two regions with high velocity gradient were appeared in the vicinity of the center of the chamber. A region extends towards the overflow weir, from $\theta=180$ to 270 degree. Another region extends towards the inlet jet from $\theta=0$ to 180 degree. The absolute value of radial velocity in two regions is increased towards the central orifice. Close to the inlet, it was increased to 33% of the maximum tangential velocity in vicinity of the central flushing orifice. However, close to the overflow weir and at $\theta=225$, it was increased to 54% of the maximum tangential velocity. It is obvious that this region is formed as result of overflow weir. Additionally a region with inward velocity was formed close to the periphery wall of the chamber from $\theta=150$ to 315° . It can be seen that this region extends to the weir position at $\theta=225$ degree (Fig. 6a).

Radial Velocity Distribution at H = 0.18R Horizontal Flow Levels

At depth level equal to 0.18R, the regions with high radial velocity, which were discussed in the previous section, are still close to the center of chamber but they moved slightly from their previous positions. The maximum outward velocity in vicinity of the central orifice and close to the overflow weir increased to 44% of the maximum tangential velocity. The other region with inward velocity close to the inlet is also extended in clockwise direction towards the inlet channel but its maximum inward

velocity was in vicinity of the central flushing orifice and it was 23% of the maximum tangential velocity. Another region with streamline tendency towards the center of chamber which was located near the basin's periphery from $\theta = 150$ to 315 degree, is now divided into two regions in this depth level. The first one is located from $\theta = 100$ to 190 degree and it was formed as a result of near bed vortex close to the inlet jet. The second one is located near the overflow weir, from $\theta = 235$ to $\theta = 315$ degree (Fig. 6b).

Radial Velocity Distribution at H = 0.28R Horizontal Flow Level

At this depth level, where the inlet jet is very active, it is obvious that the tendency of streamlines in the level is towards the center of chamber, particularly near the inlet jet ($\theta = 0$ degree). A region with high outward velocity is located near the weir but comparing to the previous height (h = 0.18R) it expands slightly towards the inlet channel in clockwise direction and its maximum outward velocity increased to 47% of the maximum tangential velocity. The other one is a small region at $\theta = 315$ degree. It can be seen that at this height the maximum inward velocity occurred close to the inlet orifice ($\theta = 0$ degree) and it was increased to 51% of the maximum tangential velocity (Fig. 6c).

Radial Velocity Distribution at H = 0.38R Horizontal Flow Levels

This horizontal plane is located at the middle of the inlet jet and at this height velocities are influenced strongly by the inlet jet. Comparing with the h=0.28R, the region with streamline tendency towards the center of chamber is increased. At this level, similar to the previous levels, two regions with high velocities exist at the center of the chamber. However, the region with outward velocity is slightly extended towards the overflow weir and its maximum value increased to 38% of the maximum tangential velocity. Therefore, the plane with highest tendency towards the center of chamber is located at the middle of the inlet jet and its maximum inward velocity occurred close to the inlet orifice which is 46% of the maximum tangential velocity (Fig. 6d).

Radial Velocity Distribution at H = 0.48R Horizontal Flow Levels

At this horizontal level, which is located at the upper part of inlet jet, the tendency of the streamlines towards the center of chamber is decreased. In contrast to the previous flow levels, the intensity of the velocity gradient in vicinity of the central air core is decreased. The maximum outward velocity is 23% of the maximum tangential velocity and the maximum inward velocity in vicinity of the inlet orifice is 45% of the maximum tangential velocity (Fig. 6e).

Radial Velocity Distribution at H = 0.58R Horizontal Flow Levels

At this flow level, which is located close to the water surface, the area with outward velocity or streamline tendency towards the periphery of chamber is developed and occupied half of the section. Additionally an outward velocity can be observed in the upper part of the inlet jet. It is formed as result of the performance of the upper inlet jet vortex close to the water surface. The maximum outward and inward velocities are occurred in vicinity of the central air core at the center of the chamber and they are 23 and 34% of the maximum tangential velocity, respectively (Fig. 6f).

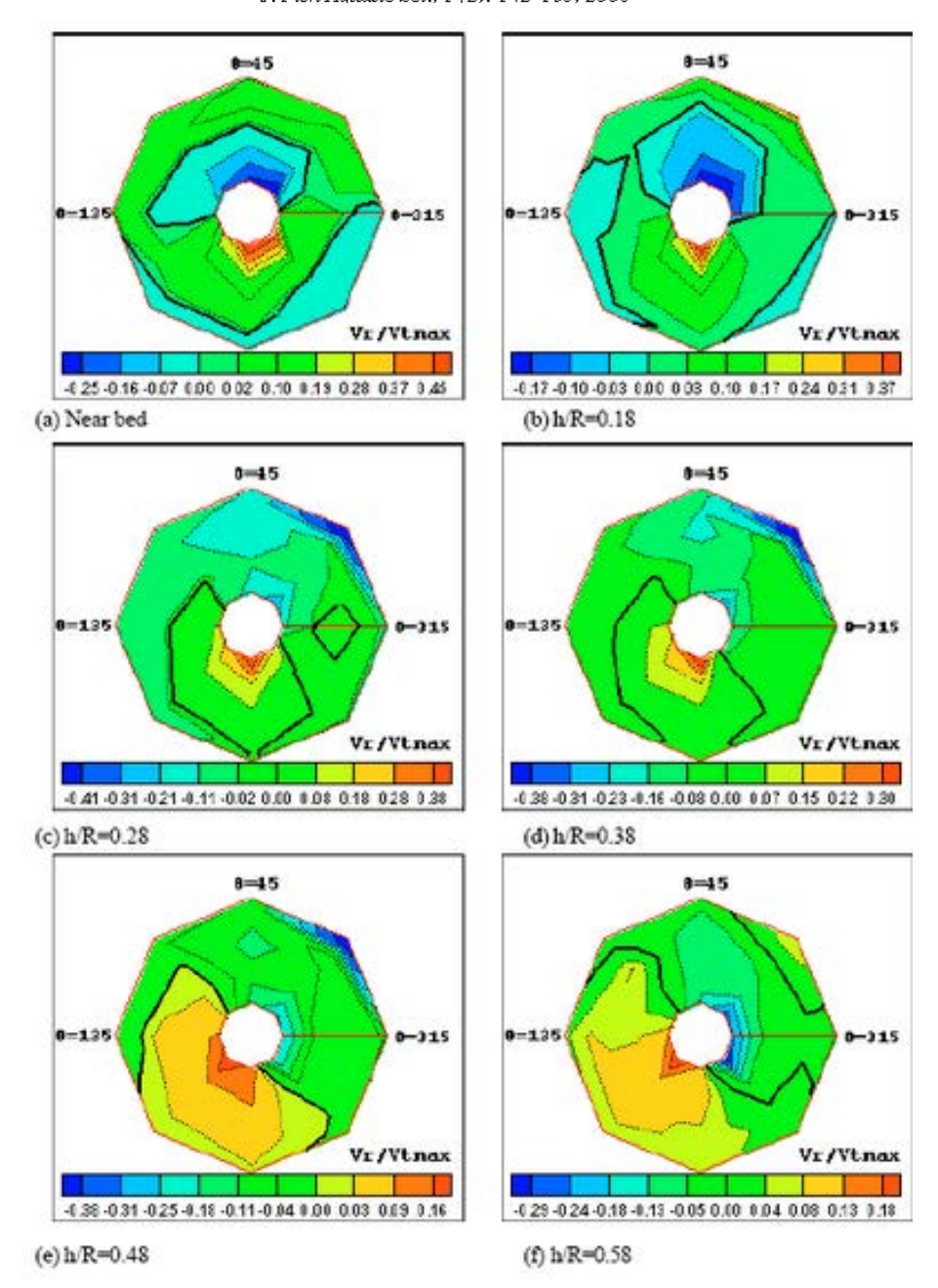


Fig. 6: The radial velocity distribution at different horizontal flow levels

Distribution of Vertical Velocity at Different Horizontal Flow Levels Vertical Velocity Distribution near the Bed

Vertical velocity distribution with anti-symmetrical pattern was found in the vicinity of the central flushing orifice. A region with upward velocities was also found from $\theta = 135$ to $\theta = 315$ degree in the lower part of the flow as it is shown in Fig. 7a. In this region the value of upward velocities increased to 12% of the maximum tangential velocity in the vicinity of the central flushing orifice. Additionally, a region with downward velocities was found from $\theta = 315$ to $\theta = 135$ degree at the upper part of the Fig. 7a. Similar to the lower part, the value of upward velocities increased towards the central flushing orifice and the velocity was about 6% of the maximum tangential velocity in the vicinity of the central flushing orifice. Unexpectedly it showed that in the vicinity of the central flushing orifice, the upward velocities are more intensive than the downward velocities. Two narrow regions were recognized in the next of periphery wall of the chamber as it is shown in the upper and lower part of the Fig. 7a. The first region is located from $\theta = 0$ to $\theta = 135$ degree close to the periphery wall of the chamber with upward velocities. This region is formed as the result of the performance of the bottom vortex which was originated from the inlet jet. As discussed previously, this vortex has upward streamlines in the next of periphery wall of the chamber. The second region was found in lower part from $\theta = 160$ to $\theta = 135$ degree and next to the periphery wall of the chamber with downward velocities. This region is formed as a result of approaching the upper inlet jet vortex to the basin floor and forming the vortex under the overflow weir currents, as the inlet jet weakens and the third vortex forms when the weir is approached. As shown previously, the upper inlet jet vortex and the vortex which is formed under the overflow weir currents have downward streamlines close to the periphery wall of the chamber (Fig. 7a).

Vertical Velocity Distribution at H = 0.18R Horizontal Flow Level

Comparing this horizontal level with the near bed section, the region with downward velocities is extended in anticlockwise direction toward the weir. Additionally the two regions with high upward and downward velocities in vicinity of the central orifice were disappeared. Both of the maximum upward and downward velocities are 14% of the maximum tangential velocity. The maximum upward velocity occurred in the next of the periphery wall of the chamber at $\theta = 45$ degree, but the maximum downward velocity occurred close to the inlet orifice at $\theta = 0$ degree (Fig. 7b).

Vertical Velocity Distribution at H = 0.28R Horizontal Flow Level

At this flow depth, which is located at the lower part of the inlet jet, the downward tendency near the basin's periphery which was located in vicinity of the overflow weir was disappeared. But some new downward velocities is formed from $\theta = 135$ to 200 degree next to the periphery wall of the chamber. This is formed as a result of upper inlet jet. The maximum upward and downward velocities of this height are 8 and 5% of the maximum tangential velocity, respectively (Fig. 7c).

Vertical Velocity Distribution at H = 0.38R to 0.58R Horizontal Flow Level

At horizontal level equal to h = 0.38R which is located at the inlet jet level. The region with upward velocities, which relates to the upper inlet jet vortex, is developed through the entire parts of the chamber. A region with downward velocities is located very close to the center of chamber. It is very small in size and finally in the subsequent levels, it will encompass the central air core completely (Fig. 7d-f).

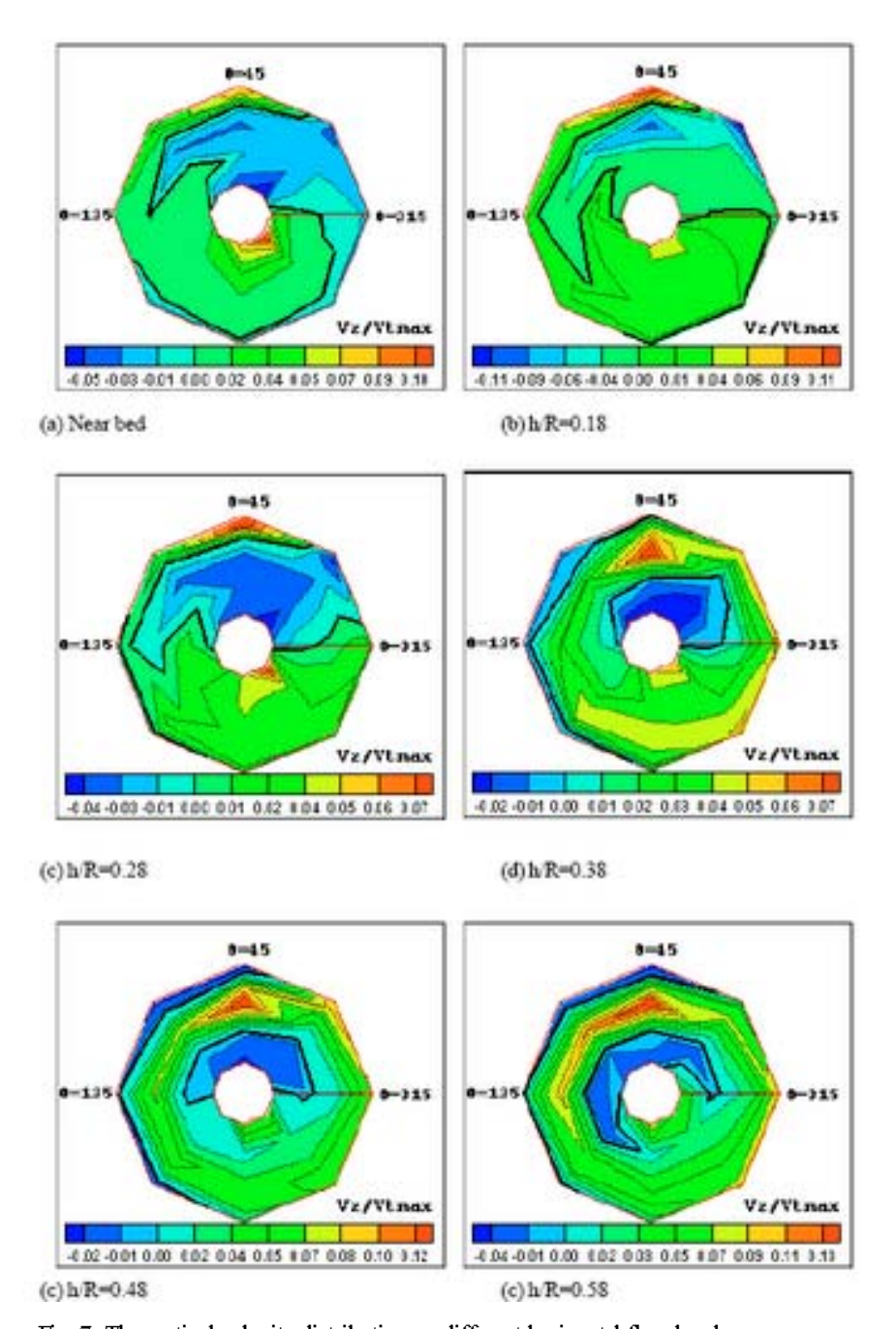


Fig. 7: The vertical velocity distribution on different horizontal flow levels

Conclusions

In this study a comprehensive study is conducted to find the flow structure in the whole domain and at each section of vortex chamber in a physical model. The velocity of flow was measured at each point of flow in three dimensions using Acoustic Doppler Velocity meter. The experiments were conducted in a circular chamber with inlet and outlet flow in anticlockwise flow condition. It was found that the most dominant secondary current within the chamber is the flow current towards the overflow weir. This secondary current occupies a region near the overflow weir, with the highest value of velocity near the bed next to the central orifice. By getting far from the bed this region extends towards the inlet channel in the opposite of the flow direction. It also stretches towards the central air core at the center of the basin. This region causes the flow currents to get away from the central air core. Therefore a region with high tendency towards the central air core will form exactly in the other side of basin, exactly similar to the region which was formed near the overflow weir but, with tendency towards the central air core. In this new region the highest tendency is occurred near the bed, especially near the central orifice. This region causes the inlet jet to deflect towards the central air core. This deflection generates two vortices. One of them forms under the inlet jet, near the bed. The other one is placed above the inlet jet. These two vortices go ahead along the inlet jet but gradually the upper vortex, by approaching towards the overflow weir comes down and also overcome the near bed vortex. This vortex through passing under the overflow weir will strengthen and make a current towards the central air core near the bed and a current with downward tendency near the periphery wall of chamber.

Acknowledgements

We thank to Professor Roland W. Jeppson, from Utah State University for his comments and careful reading of the manuscript.

References

- Athar, M., U.C. Kothyari and R.J. Garde, 2003. Distribution of sediment concentration in the vortex chamber type sediment extractor. J. Hyd. Res., 41: 427-438.
- Cecen, K. and M. Bayazit, 1975. Some laboratory studies of sediment controlling structures. calculation of load-controlling water intake structures for mountain rivers. Proceedings of the Ninth Congress of the ICID, Moscow, Soviet Union, pp. 107-110.
- Chrysostomou, V., 1983. Vortex-type settling basin. Thesis presented to the University of Southampton, at Southampton, England, in partial fulfillment of the requirements for the degree of M.Sc Thesis.
- Curi, K.V., I.I. Esen and S.G. Velioglu, 1979. Vortex type solid liquid separator. Prog. Water Technol., 7: 183-190.
- Hite, J.E. and W.C. Mih, 1994. Velocity air core vortices of Hydraulic intakes. J. Hydr. Engrg. ASCE. 120: 284-297.
- Julien, P.Y., 1986. Concentration of very fine silts in a steady vortex. JHR, Proc. IAHR, 24: 255-264.
 Mashauri, D.A., 1986. Modeling of vortex settling basin for primary clarification of water.
 Ph. D Thesis. Tampare University of Tech. Finland.
- Odgaard, A.J., 1986. Free-surface air core vortex. JHE, Proc. ASCE, 112: 610-620.

- Ogihara, K., S. Sakaguchi, 1984. New system to separate the sediment from the water flow by using the rotating flow. Proc. of 4th Congress of the Asia and Pacific Div., Intl. Assoc. Hydr. Res. Chiang Mai, Thailand, pp: 753-766.
- Paul, T.C., S.K. Sayal V.S. Sakhanja and G.S. Dhillon, 1991. Vortex settling basin design considerations. J. Hydr. Engrg. ASCE., 117: 172-189.
- Rea, Q., 1984. Secondary currents within the circulation chamber sediment extractor. MSc thesis, University of Southampton, Southampton, England.
- Salakhov, F.S., 1975. Rotational design and methods of hydraulic calculation of load-controlling water intake structures for mountain rivers. Proceedings of Ninth Congress of the ICID, Moscow, Soviet Union, pp: 151-161.
- Sullivan, R.H., 1972. The swirl concentrator as a combined sewer over-flow regulatory facility. Report No: EPA-R2-72-008, U.S. Environmental Protection Agency, Washington DC.
- Vatistas, G.H., 1989, Analysis of fine particles concentration in combined vortex. JHR, Proc. IAHR, 27: 417-426.
- Zhou, Z., J. Hou and Yi. Tang, 1997. Flow field measurement of sand funnel and its influence on sediment transport. Proc., 27th Congress, IAHR, San Fransisco.